Acta Chemica Scandinavica A 38 (1984) 711–717

Magnetic and Structural Properties of Transition Metal Substituted MnP. III. $Mn_{1-t}Fe_tP$ ($0.00 \leqq t \leqq 0.30$)

HELMER FJELLVÅG,[a] ARNE KJEKSHUS[a] and ARNE F. ANDRESEN[b]

[a] Kjemisk Institutt, Universitetet i Oslo, Blindern, N-0315 Oslo 3, Norway and
[b] Institutt for Energiteknikk, Kjeller, Norway

$Mn_{1-t}Fe_tP$ is studied for $0.00 \leqq t \leqq 0.30$ by X-ray and neutron diffraction and magnetic susceptibility measurements at temperatures between 10 and 1000 K. $Mn_{1-t}Fe_tP$ takes the MnP type structure in para-, ferro- or helimagnetic states under these conditions. The results are discussed in relation to other information on $Mn_{1-t}Fe_tP$ and related phases.

In continuation of the series of papers[1-3] on the structural and magnetic properties of the pseudo-binary $Mn_{1-t}T_tP$ phases (T=transition metal), we here give an account of results for T=Fe. The magnetic nature of $Mn_{1-t}Fe_tP$, as probed by magnetic susceptibility and magnetization measurements, is displayed in Refs. 1, 4–6. The former article[1] includes a brief summary of the same diffraction data as are presented here.

The magnetic phase diagrams for the MnP–FeP system disclosed in Refs. 1, 4, 6 harmonize, although there are slight differences in the positioning of the phase boundaries. The prominent features of this phase diagram are a para- (P), ferro- (F), helimagnetic (H_c) triple point at $t \approx 0.12$ and a continuous H_c region (*viz.* $0.00 \leqq t \leqq 1.00$) at low temperatures. The present contribution concerns only the MnP rich part of $Mn_{1-t}Fe_tP$ ($0.00 \leqq t \leqq 0.30$) and temperatures $\leqq 293$ K.

EXPERIMENTAL

Samples were made from initial batches of MnP and FeP, preparational details concerning the former being given in Ref. 2. FeP was synthesized by heating stoichiometric quantities of the elements (turnings from rods of 99.999 % Fe, Johnson, Matthey & Co. and lumps of red 99.999 % P, Koch-Licht Laboratories) in evacuated, sealed, double quartz tubes. These were placed in horizontally positioned furnaces and the temperature was slowly increased (3×20 °C per d) to 950 °C, kept there for 2 d and cooled to room temperature over 1 d. After careful grinding the samples were reheated at 1000 °C for 5 d and then slowly cooled to room temperature. The binary compounds were mixed in proportions appropriate to the desired ternary compositions. They were further subjected to two or three heat treatments (intermediate grindings) at 950 °C for 5 d, and finally cooled to room temperature over 1 d.

Experimental details concerning powder X-ray and neutron diffraction and magnetic susceptibility measurements are given in Ref. 7. The nuclear neutron scattering lengths (in 10^{-12} cm) $b_{Mn}=-0.37$, $b_{Fe}=0.95$ and $b_P=0.51$ were taken from Ref. 8, and the magnetic form factor for Mn^{2+} from Ref. 9.

RESULTS AND DISCUSSION

(i) *Atomic arrangement.* According to Bonnerot *et al.*[5] $Mn_{1-t}Fe_tP$ forms a continuous solid solution phase, with the MnP type structure, over the entire range of $0.00 \leqq t \leqq 1.00$. This finding has been confirmed for $0.00 \leqq t \leqq 0.30$ by the powder X-ray and neutron diffraction data collected in the present study. The generally sharp Bragg reflections and the absence of additional superstructure peaks in the diffraction diagrams substantiate that Mn and Fe are long range distributed at random over the metal sub-lattice.

0302-4377/84 $2.50

Table 1. Unit cell dimensions and positional parameters with standard deviations for $Mn_{1-t}Fe_tP$ as derived by Rietveld analysis of powder neutron diffraction data. Space group *Pnma*; Mn/Fe in 4*c* and P in 4*c*. (Nuclear R_n-factors ranging between 0.03 and 0.08; magnetic R_m-factors ranging between 0.04 and 0.08; profile R_p-factors ranging between 0.09 and 0.14; 20–25 nuclear reflections.)

t	T (K)	*a* (pm)	*b* (pm)	*c* (pm)	x_T	z_T	x_P	z_P
0.05	293	525.45(5)	317.10(3)	591.57(6)	0.0095(15)	0.2009(13)	0.1865(11)	0.5727(8)
	70	523.35(5)	317.49(3)	589.32(5)	0.0087(16)	0.2011(13)	0.1864(10)	0.5724(8)
	10	523.35(5)	317.42(3)	587.17(6)	0.0076(17)	0.2011(15)	0.1857(10)	0.5729(8)
0.10	293	524.92(5)	316.45(3)	590.43(7)	0.0067(19)	0.1986(25)	0.1878(10)	0.5700(8)
	220	523.97(5)	316.94(3)	589.67(5)	0.0088(18)	0.2002(15)	0.1868(9)	0.5719(7)
	100	523.18(8)	317.21(4)	588.81(9)	0.0056(28)	0.1996(30)	0.1881(12)	0.5710(9)
	10	523.21(8)	317.24(4)	588.61(9)	0.0061(31)	0.1986(31)	0.1881(14)	0.5702(10)
0.20	293	524.40(7)	315.97(4)	589.19(8)	0.0067(42)	0.1962(33)	0.1874(9)	0.5705(8)
	10	522.85(8)	316.61(4)	587.45(8)	0.0054(47)	0.1985(30)	0.1888(10)	0.5709(9)
0.28	293	523.57(13)	315.26(7)	588.19(13)	0.0050[a]	0.1980[a]	0.1889(15)	0.5709(13)
	10	522.14(13)	315.88(6)	586.95(12)	0.0050[a]	0.1980[a]	0.1857(27)	0.5727(12)

[a] Fixed in final refinements.

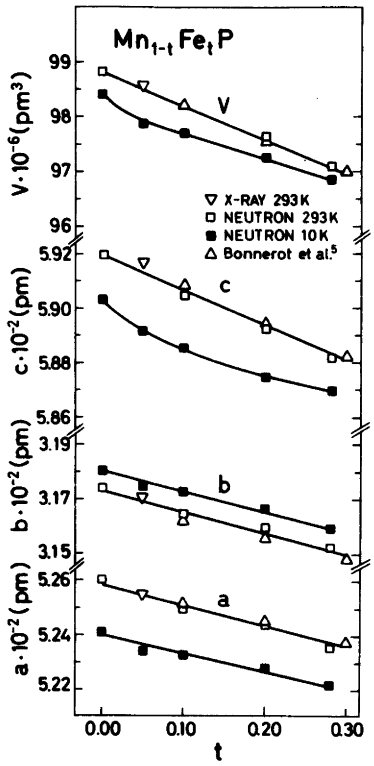

Fig. 1. Unit cell dimensions of $Mn_{1-t}Fe_tP$ *versus* t ($0.00 \leqq t \leqq 0.30$) at 10 and 293 K. Legends to symbols are given on the illustration. *Calculated* error limits do not exceed twice the size of symbols. (1 Å=10^2 pm.)

The unit cell dimensions and positional parameters (as derived from powder neutron diffraction data, and in terms of the *Pnma* space group setting, $c>a>b$, for the MnP type structure) are listed in Table 1.

The positional parameters of $Mn_{1-t}Fe_tP$ (Table 1) stay constant within two calculated standard deviations for $0.00 \leqq t \leqq 0.28$ and $10 \leqq T \leqq 293$ K. (It should be noted that the final Rietveld analyses for $Mn_{0.72}Fe_{0.28}P$ were executed with fixed values for x_T and z_T due to the small average metal scattering length.) The constancies and the numerical values of the positional parameters are consistent with a geometrical model [10,11] for the MnP type structure, and the findings [2,3,12,13] for other $Mn_{1-t}T_tP$ phases. Some implications of the constancies of the positional parameters are discussed in Ref. 3.

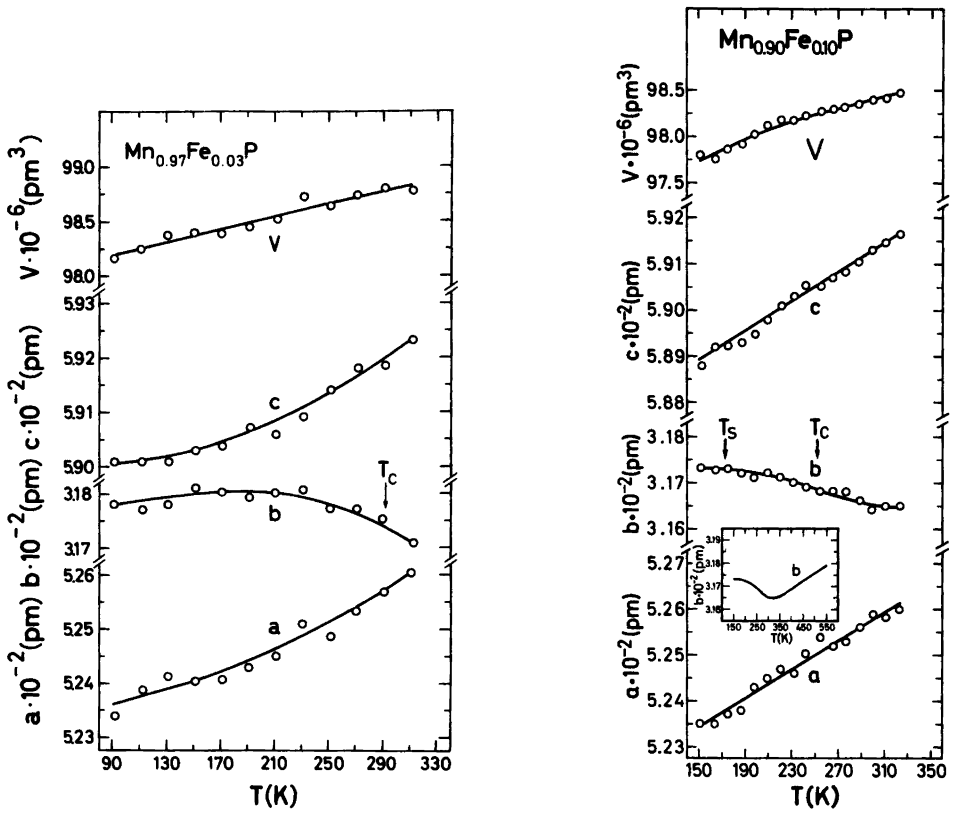

Fig. 2. Unit cell dimensions *versus* temperature (T<310 K) for (a) $Mn_{0.97}Fe_{0.03}P$ and (b) $Mn_{0.90}Fe_{0.10}P$. *Calculated* error limits do not exceed size of symbols. (1 Å=10^2 pm.) T_C and T_S refer to the P⇄F and F to H_c transition temperatures, respectively, given in (iii).

The variations of the unit cell dimensions of $Mn_{1-t}Fe_tP$ with t ($0.00 \leqq t \leqq 0.30$) at 10 and 293 K are shown in Fig. 1. The illustration includes also the results of Bonnerot *et al.*[5] which are seen to be in excellent agreement with those obtained in this study. In line with the findings[2,3,12,13] for other $Mn_{1-t}T_tP$ phases, the b axis of $Mn_{1-t}Fe_tP$ is subject to expansion between 293 and 10 K. This phenomenon, which concerns the entire composition range studied for $Mn_{1-t}Fe_tP$, originates from the magnetostriction associated with the transformation from a P to an F and/or H_c state (*cf.* the magnetic phase diagrams in Refs. 1, 4).

The temperature variations of the unit cell dimensions of $Mn_{0.97}Fe_{0.03}P$ and $Mn_{0.90}Fe_{0.10}P$ between 90 and 310 K (Fig. 2) may serve as representative examples of the results obtained for various compositions of $Mn_{1-t}Fe_tP$. The P⇄F transition temperature estimated from the kink points on the thermal expansion curves for b are consistently appreciably higher (30–60 K) than θ or T_C from magnetic susceptibility [see (ii)], neutron diffraction [see (iii)] and magnetization[1] measurements (*cf.* Refs. 2, 3, 7, 12). No or just a very weak indication of the F to H_c or P⇄H_c transitions [at T_S or T_N; see (iii) and Refs. 1, 4, 6] is observed in the present thermal expansion curves for $Mn_{1-t}Fe_tP$.

(ii) *Magnetic susceptibility.* The reciprocal magnetic susceptibility *versus* temperature data for $Mn_{1-t}Fe_tP$ with $0.00 < t \leqq 0.28$ (Fig. 3) obey the Curie-Weiss law [$\chi^{-1}=C^{-1}(T-\theta)$]. The paramagnetic moment ($\mu_{eff}=[8C_{mol}]^{1/2}$) and Weiss constant ($\theta$) are given in Table 2 together with the corresponding number of unpaired spins ($2S$) according to the "spin only" approximation

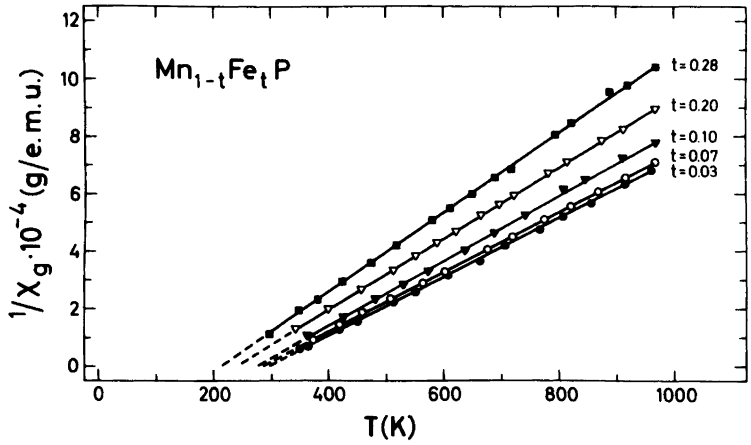

Fig. 3. Inverse magnetic susceptibility as function of temperature for $Mn_{1-t}Fe_tP$ with t=0.03, 0.07, 0.10, 0.20 and 0.28.

($\mu_{eff}=g[S(S+1)]^{1/2}$ with $g=2$). In line with the findings for the other $Mn_{1-t}T_tP$ phases, $Mn_{1-t}Fe_tP$ shows a decrease in θ, μ_{eff} and $2S$ with increasing t.

As is usually the case for P to F transitions, the θ values for $Mn_{1-t}Fe_tP$ with $0.00<t\leqq0.10$ match the Curie temperatures (T_C) found by neutron diffraction and/or magnetization measurements [see (iii) and Ref. 1]. On the other hand, in the domain of the P⇄H_c transition ($0.10<t\leqq0.28$) θ takes a higher value than the Néel temperature (T_N) established by neutron diffraction [see (iii)]. Also in these respects there is conformity with the findings[2,3,12,13] for the other $Mn_{1-t}T_tP$ phases.

A comparison between $2S$ and the magnetic moments found by neutron diffraction and magnetization measurements [see (iii) and Ref. 1] is given in Fig. 4, which also includes $2S$ values calculated from the C_{mol} *versus* t plot of Iwata *et al.*[6] The illustration shows a quite good agreement between the extrapolated magnetization moments and results (μ_F and/or μ_H) obtained by neutron diffraction. The distinction between the magnetization moments at 89 kOe and the extrapolated values is also clearly noticeable in Fig. 4. As for the other $Mn_{1-t}T_tP$ phases the paramagnetic $2S$ values are considerably higher than the ordered moments. The different sets of results for the present samples fall on approximately parallel lines which decline with increasing t. However, the $2S$ *versus* t relationship deduced from the data of Iwata *et al.*[6] differs from that for the present samples, and this disparity probably reflects the different sample preparation procedures used in the two studies (*cf.* Ref. 1). A more detailed discussion of these findings will be given in relation to the corresponding data for all $Mn_{1-t}T_tP$ phases.

(iii) *Magnetic structures.* According to Refs. 1, 4, 6 the magnetic phase diagram for $Mn_{1-t}Fe_tP$

Table 2. Weiss constant (θ), paramagnetic moment (μ_{eff}) and number of unpaired spins ($2S$) for $Mn_{1-t}Fe_tP$.

t	θ (K)	μ_{eff} (μ_B per T)	$2S$ (per T)
0.03	301±5	2.60±0.05	1.79±0.04
0.05	295±5	2.58±0.05	1.79±0.04
0.07	291±5	2.57±0.05	1.76±0.04
0.10	275±5	2.47±0.05	1.67±0.04
0.20	240±5	2.35±0.05	1.56±0.04
0.28	213±5	2.22±0.05	1.44±0.04

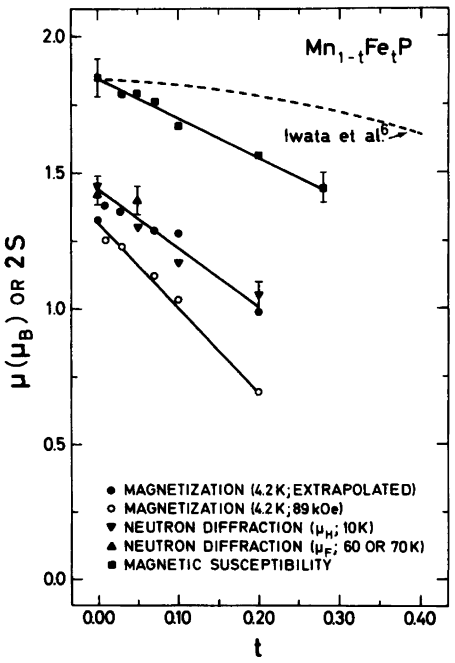

Fig. 4. Paramagnetic ("spin only") 2*S* values and magnetic moments from magnetization (89 kOe and extrapolated data; Ref. 1) and neutron diffraction (μ_F and μ_H) measurements *versus* the compositional parameter *t*. Legends to symbols are given on the illustration. Bars represent estimated or calculated errors.

with $0.00 \leqq t \leqq 1.00$ and $0<T<300$ K includes the P, F and H_c phases which meet in a triple point at $t \approx 0.12$.

The present neutron diffraction results confirm the existence of the F phase for $t=0.05$ and 0.10 with, respectively, $T_C=280\pm5$ and 250 ± 5 K, $T_S=63\pm5$ and 173 ± 15 K and $\mu_F=1.40(5)$ μ_B at 70 K and ~0.8 μ_B at 220 K. (The direction of the ferromagnetic moments is parallel to *b* for $t=0.05$, whereas the relatively narrow existence range of the F phase for $t=0.10$ causes some degree of ambiguity concerning the direction as well as the magnitude of the moments.)

No indication of hysteresis is observed in the temperature variation of the integrated intensity of the $000^{\pm}$ satellite for the various samples (Fig. 5). There is accordingly no distinction between $t=0.05$ and 0.10, which undergo the H_c to F transition (known[14] to be of first order for $t=0.00$), and $t=0.20$ and 0.28, which are subject to the $H_c \rightleftarrows P$ transition, in this respect. However, in line with the findings[2,3,12,13] for other $Mn_{1-t}T_tP$ phases, the temperature characteristics in Fig. 5 are rather broad.

The original model[15,16] for the magnetic structure of the H_c phase of MnP is used, since, in addition to MnP itself, this also applies as an approximation to FeP[17] and moreover appears to be consistent with the magnetization data of Iwata *et al.*[6] for $Mn_{1-t}Fe_tP$. Numerical values for the variable parameters of the model (*viz.* the propagation vector τ_c of the spirals, the helimagnetic moment μ_H and the phase angle $\phi_{1,2}$ between the spirals through atoms 1 and 2, *cf.* Ref. 7) are given in Table 3, which also includes the corresponding results for MnP (powder data, *cf.* the discussion in Ref. 2) and FeP (single crystal data[17]) for comparison.

The compositional variations of τ_c, μ_H and $\phi_{1,2}$ at 10 K are seen from Table 3 (an illustration is included in Ref. 1), which reveals appreciable variations in τ_c and μ_H with *t*, whereas $\phi_{1,2}$ is approximately concentration independent for $0.00 \leqq t \leqq 0.28$. The latter observation is very interesting in view of the thus required large

Table 3. Helimagnetic parameters for $Mn_{1-t}Fe_tP$ at 10 K. (R_{spiral} ranging between 0.04 and 0.09; 7–12 magnetic satellite reflections.)

t	$\tau_c/2\pi c^*$	μ_H (μ_B)	$\phi_{1,2}$ (°)	T_S (K)	T_N (K)
0.00	0.116±0.002	1.45±0.04	24±3	53±3	
0.05	0.113±0.003	1.30±0.05	33±5	63±3	
0.10	0.147±0.003	1.17±0.05	35±5	173±15	
0.20	0.213±0.005	1.05±0.08	20±10		210±15
0.28	0.260±0.008	0.72±0.14	30±20		175±10
1.00[a]	0.20	0.41(av.)	168.8		125±1

[a] Single crystal data quoted from Ref. 17.

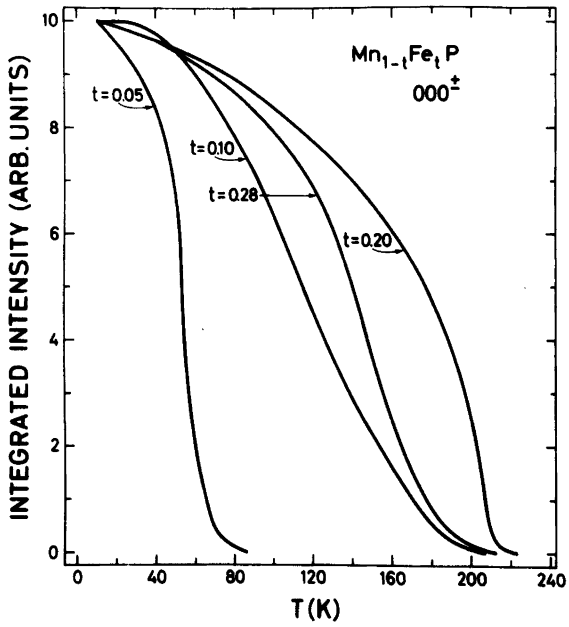

Fig. 5. Integrated intensity of $000^{\pm}$ *versus* temperature for $Mn_{1-t}Fe_tP$ with t=0.05, 0.10, 0.20 and 0.28. (H_c transforms to F for t=0.05 and 0.10 and to P for t=0.20 and 0.28.) Experimental points are omitted for clarity.

jump in $\phi_{1,2}$ from ~30° for t=0.28 to 168.8° for t=1.00. According to the complete chemical solid solubility of the $Mn_{1-t}Fe_tP$ phase[5] and the continuous variation of T_N [as determined from the maximum in the χ(T) curves of Iwata *et al.*[6]] with t for $\sim 0.12 \leqq t \leqq 1.00$, one is led to believe that the magnetic solid solubility of the H_c phase covers the entire range $0.00 \leqq t \leqq 1.00$ below 50 K. While the trends in the changes of τ_c and μ_H with t can easily be visualized to comply with this picture, the situation for $\phi_{1,2}$ gives rise to strong doubts. However, in order to check the possible existence of a magnetic two-phase region between MnP and FeP rich H_c phase regions, additional samples and neutron diffraction experiments are needed. The necessary syntheses have been started and we intend to report on this aspect in a forthcoming paper.

The satellite reflections of all $Mn_{1-t}Fe_tP$ samples are generally broader (*viz.* as judged by their half-widths) than the corresponding nuclear (or combined nuclear and ferromagnetic) reflections. The same observation was made for $Mn_{1-t}V_tP$,[3] whereas this feature was not noticed for the other $Mn_{1-t}T_tP$ phases[2,12,13] we have studied. Since $Mn_{1-t}V_tP$ and $Mn_{1-t}Fe_tP$ also distinguish themselves by appreciable compositional variations in τ_c, it is suggested that the broadening of the satellites originates from the inevitable, local fluctuations in the Mn–T distribution within powder samples prepared by solid state reactions.

Bertaut[18] has proposed correlation between the mutual influence of pressure, chemical substitution, transition temperatures and volume changes for phases with the MnP type structure. Since the compositional variations of T_S, T_N and $V2tFe_tP$ are used as a specific example in Bertaut's considerations it is tempting to raise a discussion here. However, the shortcoming of this approach becomes more evident when the data for all $Mn_{1-t}T_tP$ phases (which we have studied) are taken into account. The discussion is therefore postponed.

The temperature dependences of τ_c for t=0.00, 0.05, 0.10, 0.20 and 0.28 are shown in Fig. 6. Except for the sample with t=0.05 (with T_S=63±3 K and T_C=280±5 K) μ_H is found to decrease with increasing T, μ_H being reduced to zero at T_N for t=0.20 and 0.28. Due to the close coupling between μ_H and $\phi_{1,2}$, the situation for $\phi_{1,2}$ is less clear, but the present data for

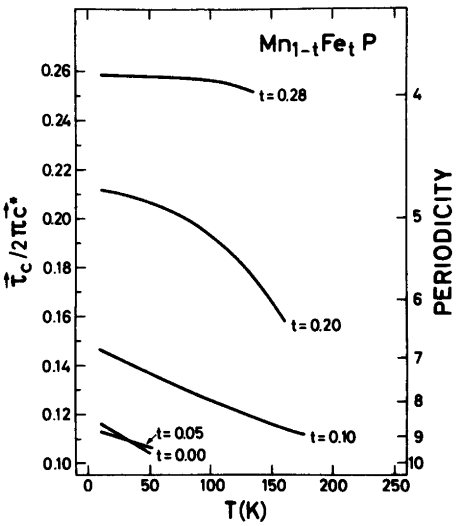

Fig. 6. Temperature dependences of the propagation vector (τ_c) for $Mn_{1-t}Fe_tP$ with t=0.00, 0.05, 0.10, 0.20 and 0.28. Experimental points are omitted.

$Mn_{1-t}Fe_tP$ appear to suggest that $\phi_{1,2}$ is an essentially temperature independent parameter.

REFERENCES

1. Fjellvåg, H., Kjekshus, A., Zięba, A. and Foner, S. *J. Phys. Chem. Solids 45* (1984) *In press*.
2. Fjellvåg, H. and Kjekshus, A. *Acta Chem. Scand. A 38* (1984) 563.
3. Fjellvåg, H. and Kjekshus, A. *Acta Chem. Scand. A 38* (1984) 703.
4. Roger, A. and Fruchart, R. *C. R. Acad. Sci. C 264* (1967) 508.
5. Bonnerot, J., Fruchart, R. and Roger, A. *Phys. Lett. A 26* (1968) 536.
6. Iwata, N., Fujii, H. and Okamoto, T. *J. Phys. Soc. Jpn. 46* (1979) 778.
7. Fjellvåg, H. and Kjekshus, A. *Acta Chem. Scand. A 38* (1984) 1.
8. Bacon, G. E. In Yelon, W. B., Ed., *Neutron Diffraction Newsletter,* Columbia 1977.
9. Watson, R. E. and Freeman, A. J. *Acta Crystallogr. 14* (1961) 27.
10. Selte, K. and Kjekshus, A. *Acta Chem. Scand. 27* (1973) 3195.
11. Endresen, K., Furuseth, S., Selte, K., Kjekshus, A., Rakke, T. and Andresen, A. F. *Acta Chem. Scand. A 31* (1977) 249.
12. Fjellvåg, H., Kjekshus, A. and Andresen, A. F. *Acta Chem. Scand. A 39* (1985). *In press*.
13. Fjellvåg, H. and Kjekshus, A. *Acta Chem. Scand. A 38* (1984). *In press*.
14. *Gmelins Handbook of Inorganic Chemistry, System No. 56: Mangenese, Vol. C 9,* Berlin–Heidelberg–New York 1983.
15. Felcher, P. G. *J. Appl. Phys. 37* (1966) 1056.
16. Forsyth, J. B., Pickart, S. J. and Brown, P. J. *Proc. Phys. Soc. 88* (1966) 333.
17. Felcher, P. G., Smith, F. A., Bellavance, D. and Wold, A. *Phys. Rev. B 3* (1971) 3046.
18. Bertaut, E. F. *Pure Appl. Chem. 52* (1979) 73.

Received April 12, 1984.